Computer Analysis of Imperfection Sensitivity of Ring-Stiffened Orthotropic Shells of Revolution

GERALD A. COHEN*
Structures Research Associates, Laguna Beach, Calif.

A formulation suitable for digital computer solution of Koiter's unique mode stability theory is presented for ring-stiffened, orthotropic, multilayered shells of revolution subjected to axisymmetric torsionless loads. Both nonlinear prebuckling states and live pressure loadings are treated. The boundary value problem for the second-order contribution to the postbuckling state is based on Novozhilov-type nonlinear moderate rotation shell and ring theory. In general, the second-order state consists of an axisymmetric component and an unsymmetric harmonic component, each of which are obtained by the forward integration method using the Runge-Kutta numerical technique. The associated postbuckling and imperfection functionals are then obtained by quadrature over the shell and rings. The imperfection analysis is based on a mean square angular imperfection measure, which includes imperfections of both shell and rings. For a given value of this measure, the imperfection which produces the greatest reduction in buckling load (for sufficiently small imperfections) and the imperfection proportional to the buckling mode displacements are treated. Numerical results are presented for: 1) clamped spherical caps, 2) a simply supported stringer-stiffened cylinder, 3) a prolate spheroid, and 4) a ring-stiffened prolate spheroid. The present results are in excellent agreement with previous theoretical results, which exist for the first three problems. In addition, reasonable imperfection amplitudes may be correlated with experimental buckling loads previously obtained for the first, third, and fourth problems.

Nomenclature

A = shell surface area; also, ring or stringer cross-sectional area
a = first postbuckling coefficient; also, ring centroidal radius
b = second postbuckling coefficient
D = shell wall flexural rigidity
d = stringer spacing
E = Young's modulus for a ring or stringer
e = normal eccentricity of stringer centroid from shell middle surface
e_1,e_2,e_{12} = meridional, circumferential, and shear linearized shell strain expressions, respectively
F_x,F_y,F_ϕ = external ring forces per unit of length in axial, radial, and circumferential directions, respectively
$F^{(1)}(u_1,u_1)$ = buckling mode functional
G = shear modulus of stringer
H = shallow spherical shell rise
I = integral defined by Eq. (5); also, stringer centroidal moment of inertia
J = torsion constant for stringer section
K = postbuckling stiffness at bifurcation
k = ring index
K_0 = prebuckling stiffness at bifurcation
L_1,L_2 = external shell surface moments per unit of area about meridional and circumferential directions, respectively
l = cylindrical shell length
M_1,M_2,M_{12} = meridional, circumferential, and twisting shell stress couples, respectively
N = number of finite-difference stations
N_x,N_y,N_ϕ = external ring moments per unit of length in axial, radial, and circumferential directions, respectively
n = harmonic number
n_c = buckling mode harmonic number
P_c = critical axial load for cylindrical shell
P_0 = classical buckling load for an infinitely long unstiffened cylinder
P,Q,S = effective shell forces per unit of circumferential length in axial, radial, and circumferential directions, respectively
p = pressure distribution associated with normal pressure field $\lambda p(x,y)$
p_c = critical pressure
p_0 = classical critical pressure for complete spherical shell
p_s = snapping pressure
q = $[12(1-\nu^2)]^{1/4}(r_b/t)^{1/2}$
R = spherical shell radius
R_2 = circumferential radius of curvature
r = small circle radius
r_a = semimajor axis of spheroid
r_b = semiminor axis of spheroid
s = meridional arc distance
T_1,T_2,T_{12} = meridional, circumferential, and shear shell stress resultants, respectively
T_ϕ = ring hoop stress resultant
t = shell thickness
u,v = meridional and circumferential shell displacements, respectively (see also generalized field variables)
X,Y,Z = shell variables defined by Eqs. (6)
X_1,X_2,X_3 = external shell surface forces per unit of area in meridional, circumferential, and normal directions, respectively
Z = curvature parameter for cylindrical shell, $(l^2/rt)(1-\nu^2)^{1/2}$
α,β = first and second imperfection parameters, respectively
Δ = incremental value; also, end shortening of cylinder
Δ_c = end shortening at bifurcation load
$\bar{\delta}$ = maximum normal displacement of buckling mode imperfection
$\epsilon_1,\epsilon_2,\epsilon_{12}$ = meridional, circumferential, and shear shell stretching strains, respectively
$\kappa_1,\kappa_2,\kappa_{12}$ = meridional, circumferential, and shear shell bending strains, respectively
Λ = $2[3(1-\nu^2)]^{1/4}(H/t)^{1/2}$
λ = load factor
λ_c = critical load factor for bifurcation buckling of perfect structure

Presented at the 11th ASME/AIAA Structures, Structural Dynamics, and Materials Conference, Denver, Colo., April 1970 (no paper number; published in bound volume); submitted June 23, 1970; revision received August 27, 1970. This work was supported by NASA/LRC Contract NAS1-5554-8.

* President. Member AIAA.

λ_s = buckling load for imperfect structure (snapping load)
$\lambda_{ij}(i,j = 1,2,3,4)$ = orthotropic shell wall normal moduli defined by Eq. (7) of Ref. 20
μ = buckling mode functional defined by Eq. (8)
$u_{ij}(i,j = 1,2)$ = orthotropic shell wall shear moduli defined by Eq. (7) of Ref. 20
ν = Poisson's ratio
Θ = arc tan$(\Delta_c K/P_c)$
Θ_0 = arc tan$(\Delta_c K_0/P_c)$
ξ = perturbation parameter (contribution of the buckling mode to the postbuckling state)
ξ,η,v = shell displacements in axial, radial, and circumferential directions, respectively
$\bar{\xi}$ = root-mean-square angular imperfection amplitude
ϕ = circumferential angle
χ,ψ,θ = shell elemental rotations about circumferential, meridional, and normal directions, respectively
Ω_x,Ω_y = ring variables defined by Eqs. (6)
$\omega_x,\omega_y,\omega_\phi$ = ring elemental rotations about axial, radial, and circumferential directions, respectively

Subscripts

max = maximum value
mode = pertaining to imperfection shape proportional to buckling mode

Superscripts

$(\ )^{(e)}$ = nonhomogeneous part
$(\ )^{(0)}$ = pertaining to the prebuckling state (generally evaluated at $\lambda = \lambda_c$)
$(\ )^{(1)}$ = pertaining to the buckling mode
$(\ )^{(2)}$ = pertaining to the second-order postbuckling state
$(\tilde{\ })$ = pertaining to an arbitrary imperfection
$(\bar{\ })$ = pertaining to a normalized imperfection shape
$(\hat{\ })$ = pertaining to the imperfection shape which maximizes α
$(\ )^*$ = evaluated at $\lambda = \lambda_c$
$(\ )'$ = $\partial(\ )/\partial s$
$(\dot{\ })$ = $\partial(\ )/\partial\phi$

Generalized field variables and operators

$L_2(u)$ = quadratic operator representing the nonlinear part of the strain-displacement relations
$L_{11}(u,v)$ = bilinear operator defined by the identity $L_2(u + v) = L_2(u) + 2L_{11}(u,v) + L_2(v)$
$q_1(u)$ = perturbation load vector associated with a (live) normal pressure field
u = displacement
σ = stress

Generalized variable subscripts

0 = associated with the prebuckling state
1 = associated with the buckling mode

Matrices

$[e]$ = 4×4 ring eccentricity matrix
$[k]$ = 4×4 ring stiffness matrix
$\{L\}$ = 4×1 boundary condition load matrix
$\{y\}$ = 4×1 internal shell force matrix
$\{z\}$ = 4×1 shell displacement matrix
$[\kappa]$ = 4×4 ring prestress matrix

Matrix superscripts

$(\ )^T$ = transpose

I. Introduction

IN the recent past, a fruitful area for research in shell buckling problems has been the application to specific shell geometries of the initial postbuckling and imperfection sensitivity theory, originally developed by Koiter,[1-3] and further expounded in a somewhat more specific form by Budiansky and Hutchinson.[4-6] In general, problems based on Koiter's theory may be classified as either mode interaction problems or independent mode problems. Mode interaction problems occur when for the perfect structure, the lowest bifurcation load corresponds to a multiple eigenvalue (i.e., two or more linearly independent buckling modes exist),[1,7,8] and independent mode problems occur when the lowest buckling mode is unique.[9-16] In addition, it should be noted that the interaction of higher bifurcation modes may also become important for equilibrium states at loads out of the immediate vicinity of the critical bifurcation load.

Although, even for unique mode buckling, mode interactions may thus be necessary to extend the validity of the results out of the immediate neighborhood of the critical bifurcation load, they are not considered in this paper. The formulation and results presented are based on the independent mode analysis of Ref. 17 for each bifurcation mode of interest.

Details of the computer program, which is based on the formulation presented, may be found in the computer program document,[18] and are not presented in this paper.

As noted in Ref. 3, even when an imperfection proportional to the buckling mode is assumed, the usual imperfection measure, the ratio $\bar{\delta}/t$ of maximum normal deviation to shell thickness, can be somewhat misleading since for a given value of $\bar{\delta}/t$, thinner shells may appear to be less imperfection-sensitive. In this paper an alternate imperfection measure is used, viz., the mean square value of angular deviations of both shell and rings. For a given value of this measure, the imperfection producing the greatest loss of stability for sufficiently small imperfections is compared with the imperfection proportional to the buckling mode. Additionally, although the second imperfection parameter β introduced in Ref. 17 represents an incomplete second approximation for finite buckling load knockdowns, its effect is included in the presented results.

II. Analytical Formulation

The general theory upon which this study is based has been presented in Ref. 17. In the developnent presented there, no restrictions on the structural geometry are imposed. In this study, attention is restricted to ring-stiffened shells of revolution subjected to axisymmetric torsionless loads, and consequently, the analytical formulation is, in a sense, a specialization of the equations of Ref. 17 to this class of structures.

A. Imperfection Analysis

Imperfection measure

A primary goal of this study was to develop a capability to assess the snapping loads of stiffened shells of revolution as a function of a mean imperfection amplitude or measure $\bar{\xi}$. For this purpose it is convenient to consider geometrical imperfections as angular deviations of either shell or ring elements from the desired geometrical orientation, and $\bar{\xi}^2$ as a mean square imperfection amplitude given by†

$$\bar{\xi}^2 = \left(\frac{1}{A}\right)\int_s\int_0^{2\pi}(\tilde{\chi}^2 + \tilde{\psi}^2 + \tilde{\theta}^2)r\,d\phi\,ds + \left(2\pi\sum_k a\right)^{-1}\sum_k a\int_0^{2\pi}(\tilde{\omega}_x{}^2 + \tilde{\omega}_y{}^2)d\phi \quad (1)$$

where the integral over s ranges over the whole shell meridian, and the summations over k range over all rings. With this

† The ring angular deviation $\tilde{\omega}_\phi$ does not enter into the theory, and therefore is omitted from Eq. (1).

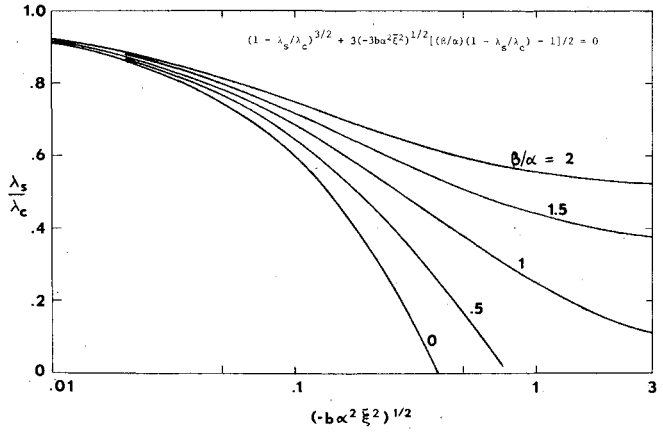

Fig. 1 Critical loads of imperfection sensitive structures.

definition of the imperfection amplitude, the relation $\tilde{u} = \bar{\xi}\bar{u}$, between the imperfection $\tilde{u}$ and the normalized imperfection shape $\bar{u}$, yields the normalization condition

$$\left(\frac{1}{A}\right)\int_s\int_0^{2\pi}(\bar{\chi}^2 + \bar{\psi}^2 + \bar{\theta}^2)rd\phi ds + \left(2\pi\sum_k a\right)^{-1}\sum_k a\int_0^{2\pi}(\bar{\omega}_x{}^2 + \bar{\omega}_y{}^2)d\phi = 1 \quad (2)$$

Except for Eq. (2) and conditions of continuity, the normalized imperfection angles, $\bar{\chi}$, $\bar{\psi}$, $\bar{\theta}$ for the shell and $\bar{\omega}_x$, $\bar{\omega}_y$ for the rings, are arbitrary functions of s and ϕ.

Snapping load

For a given imperfection shape, Eq. (35) of Ref. 17 gives the snapping load λ_s in the case where the first postbuckling coefficient a is nonzero, and Eq. (36) of Ref. 17 gives λ_s when $a = 0$ and the second postbuckling coefficient b is negative. Since for axisymmetric structures having a unique (unsymmetrical) harmonic buckling mode, a is identically zero, the latter of these two equations is of primary importance here. This equation is reproduced here as Eq. (3) and displayed graphically in Fig. 1:

$$(1 - \lambda_s/\lambda_c)^{3/2} + 3(-3b\alpha^2\bar{\xi}^2)^{1/2}[(\beta/\alpha) \times (1 - \lambda_s/\lambda_c) - 1]/2 = 0 \quad (3)$$

Equation (3) reduces to the original Koiter relation [Eq. (45.10) with $n = 4$ of Ref. 1] if β is set to zero. On the other hand, for a linear prebuckling state neglecting prebuckling deformations, $\beta = \alpha$. Therefore, β is included in an attempt to improve the accuracy of Eq. (3); however, as noted in Ref. 17, Eq. (3) is not a complete second approximation since other terms of the same order as β-terms have been neglected. In order to use Fig. 1 to determine the snapping load λ_s as a function of the root-mean-square imperfection amplitude $\bar{\xi}$, it is necessary to know the corresponding critical load λ_c and postbuckling coefficient b of the perfect structure, and the first and second imperfection parameters α and β. [It is evident that Fig. 1 cannot be used for too large a value of $\bar{\xi}$ since for $\beta/\alpha \geq 1$, as $\bar{\xi}$ becomes large, λ_s/λ_c approaches from above the asymptote $(\beta/\alpha - 1)/(\beta/\alpha)$, whereas for $\beta/\alpha < 1$, λ_s/λ_c becomes negative.] Note that all these quantities are determined for each bifurcation buckling mode of the perfect structure, each of which, therefore, has a $\lambda_s - \bar{\xi}$ relationship. The theory, to obtain each buckling mode of ring-stiffened shells of revolution, has been presented in Ref. 19, and it is assumed henceforth that λ_c and other details of the buckling mode, along with the prebuckling state at λ_c, are known inputs to the imperfection analysis.

On the other hand, if $a = 0$ and $b > 0$, Eq. (3) does not apply and the structure may carry loads greater than λ_c. In order to assess this additional load-carrying capacity, it is desirable to compute the ratio of initial postbuckling stiffness K to the prebuckling stiffness at bifurcation K_0. Formulas for the functions b, K_0, K, α, and β are presented in Ref. 17, and it is the basic purpose of this study to evaluate these quantities for each buckling mode and imperfection shape of interest.

Worst imperfection shape

As is evident from Fig. 1, for sufficiently small imperfection amplitudes, the value of β is relatively unimportant. For this reason, the worst imperfection shape, which for a given (sufficiently small) value of $\bar{\xi}$ tends to produce the greatest reduction in critical load, is defined as those particular imperfection angles, denoted here by $\hat{\chi}$, $\hat{\psi}$, $\hat{\theta}$, $\hat{\omega}_x$, $\hat{\omega}_y$, which maximize the value of α subject to the normalization condition (2).

From Ref. 17, the general expression for α is

$$\alpha = [\sigma_0{}^*\cdot L_{11}(\bar{u},u_1) + \sigma_1\cdot L_{11}(\bar{u},u_0{}^*) - \lambda_c q_1(\bar{u})\cdot u_1]/\lambda_c F^{(1)}(u_1,u_1) \quad (4)$$

Since the denominator of this expression is independent of the imperfection, it is only necessary to find the imperfection shape which maximizes the numerator. For ring-stiffened shells of revolution, the numerator, denoted here as I, is given by‡

$$I \equiv \int_s\int_0^{2\pi}(X\bar{\chi} + Y\bar{\psi} + Z\bar{\theta})rd\phi ds + \sum_k a\int_0^{2\pi}(\Omega_x\bar{\omega}_x + \Omega_y\bar{\omega}_y)d\phi \quad (5)$$

where

$$X = T_1{}^{(0)}\chi^{(1)} + T_1{}^{(1)}\chi^{(0)} - \lambda_c p u^{(1)} \quad (6a)$$

$$Y = T_2{}^{(0)}\psi^{(1)} + T_{12}{}^{(1)}\chi^{(0)} - \lambda_c p v^{(1)} \quad (6b)$$

$$Z = [T_1{}^{(0)} + T_2{}^{(0)}]\theta^{(1)} \quad (6c)$$

$$\Omega_x = T_\phi{}^{(0)}\omega_x{}^{(1)} \quad (6d)$$

$$\Omega_y = T_\phi{}^{(0)}\omega_y{}^{(1)} \quad (6e)$$

From Eq. (2) and the following Schwarz inequality,

$$I^2 \leq \mu^2\left[\left(\frac{1}{A}\right)\int_s\int_0^{2\pi}(\bar{\chi}^2 + \bar{\psi}^2 + \bar{\theta}^2)rd\phi ds + \left(2\pi\sum_k a\right)^{-1}\sum_k a\int_0^{2\pi}(\bar{\omega}_x{}^2 + \bar{\omega}_y{}^2)d\phi\right] \quad (7)$$

where

$$\mu^2 = A\int_s\int_0^{2\pi}(X^2 + Y^2 + Z^2)rd\phi ds + \left(2\pi\sum_k a\right)\sum_k a\int_0^{2\pi}(\Omega_x{}^2 + \Omega_y{}^2)d\phi \quad (8)$$

it follows that the maximum value of α is

$$\alpha_{\max} = \mu/\lambda_c F^{(1)}(u_1,u_1) \quad (9)$$

Furthermore, this value is reached only for the special imperfection angles given by

$$\hat{\chi} = AX/\mu \quad (10a)$$

$$\hat{\psi} = AY/\mu \quad (10b)$$

‡ For clarity, the asterisk is omitted from explicit prebuckling variables, it being understood that they are evaluated at λ_c. In obtaining Eq. (5), normal pressure field terms associated with surface dilatation and pressure gradients have been neglected. For dead loading, the terms in Eqs. (6a) and (6b) with the factor p should be omitted.

$$\hat{\theta} = AZ/\mu \tag{10c}$$

$$\hat{\omega}_x = \left(2\pi \sum_k a\right)\Omega_x/\mu \tag{10d}$$

$$\hat{\omega}_y = \left(2\pi \sum_k a\right)\Omega_y/\mu \tag{10e}$$

B. Perfect Structure Analysis

Whereas the imperfection parameters α and β depend only on the prebuckling state and buckling mode (which may be called the first-order postbuckling state) of the perfect structure, b and K depend, in addition, on the second-order postbuckling state. The equations for this state are given in Ref. 17 in variational form. However, for numerical purposes, the corresponding differential equations are more convenient to use, and they are most easily derived by applying the perturbation procedure directly to the nonlinear field equations.

Field equations for shells of revolution

A suitable form of the nonlinear field equations for shells of revolution is given in Sect. II of Ref. 19. Before applying the perturbation procedure, it is convenient to transform these equations to a set of eight basic differential equations in the eight basic shell variables P, Q, S, M_1, ξ, η, v, χ, plus a set of supplemental equations, as has been done previously for the linearized shell eqution (Ref. 20) and the corresponding perturbation equations (Ref. 19). The transformation of the equations is accomplished with the help of the Gauss-Codazzi surface compatibility relations. The resulting equilibrium equations are

$$(rP)' + (r/R_2)S^{\cdot} - (2/r)M_{12}^{\cdot} - (r'/r)M_2^{\cdot\cdot} - (r/R_2)[(T_1 + T_2)\theta]^{\cdot} + r'(T_2\psi + T_{12}\chi)^{\cdot} + r[(r/R_2)X_1 - r'X_3] + r'L_1^{\cdot} = 0 \tag{11a}$$

$$(rQ)' + r'S^{\cdot} - T_2 + M_2^{\cdot\cdot}/R_2 - r'[(T_1 + T_2)\theta]^{\cdot} - (r/R_2)(T_2\psi + T_{12}\chi)^{\cdot} + r[r'X_1 + (r/R_2)X_3] - (r/R_2)L_1^{\cdot} = 0 \tag{11b}$$

$$rS)' + r'S + T_2^{\cdot} + M_2^{\cdot}/R_2 - r'(T_1 + T_2)\theta - (r/R_2)(T_2\psi + T_{12}\chi) + rX_2 - (r/R_2)L_1 = 0 \tag{11c}$$

$$(rM_1)' + r[r'P - (r/R_2)Q] - r'M_2 + 2M_{12}^{\cdot} - r(T_1\chi + T_{12}\psi) + rL_2 = 0 \tag{11d}$$

The nonlinear terms in Eqs. (11) can be conveniently thought of as the following additional load terms applied to the linearized equations:

$$X_1 = -[(T_1 + T_2)\theta]^{\cdot}/r \tag{12a}$$

$$X_2 = -(r'/r)(T_1 + T_2)\theta \tag{12b}$$

$$X_3 = 0 \tag{12c}$$

$$L_1 = T_2\psi + T_{12}\chi \tag{12d}$$

$$L_2 = -(T_1\chi + T_{12}\psi) \tag{12e}$$

This isolation of the nonlinear terms is desirable since linear terms will pass through the perturbation procedure unaffected.

The four basic kinematic equations may be written in the form

$$\xi' = r'\chi + (r/R_2)e_1 \tag{13a}$$

$$\eta' = -(r/R_2)\chi + r'e_1 \tag{13b}$$

$$v' = -\xi^{\cdot}/R_2 - (r'/r)(\eta^{\cdot} - v) + e_{12} \tag{13c}$$

$$\chi' = \kappa_1 \tag{13d}$$

Equations (13) are linear since they do not involve the strains ϵ_1, ϵ_{12} but rather the linearized strain expressions e_1, e_{12}. In addition to the nonlinear strain-rotation equations, given by Eqs. (1) of Ref. 19, and the partially inverted constitutive relations, given by Eqs. (6) of Ref. 20 with S replaced by $S - (T_1 + T_2)\theta/2$, the following equations complete the transformed system of field equations

$$T_{12} = S - 2M_{12}/R_2 - (T_1 + T_2)\theta/2 \tag{14a}$$

$$T_1 = (r/R_2)P + r'Q \tag{14b}$$

$$e_2 = (\eta + v^{\cdot})/r \tag{14c}$$

$$\kappa_2 = [r'(\chi + \xi^{\cdot\cdot}/r) + (v^{\cdot} - \eta^{\cdot\cdot})/R_2]/r \tag{14d}$$

$$\kappa_{12} - e_{12}/R_2 = (\chi - \xi/r)^{\cdot}/r \tag{14e}$$

$$\psi = (v - \eta^{\cdot})/R_2 + (r'/r)\xi^{\cdot} \tag{14f}$$

$$\theta = (r'/r)(v - \eta^{\cdot}) - \xi^{\cdot}/R_2 \tag{14g}$$

Equations for second-order postbuckling state

In deriving the equations for the second-order contribution to the postbuckling state, all response variables of the postbuckling state are expanded in a power series in a parameter ξ (not to be confused with the axial displacement ξ) about the corresponding variables of the prebuckling state at the same load level λ. These expansions are then substituted directly into each of the field equations. Terms of the same order in ξ are collected after subtracting off the corresponding equations satisfied by the prebuckling state variables. Terms of order ξ then yield the buckling mode (eigenvalue) equations and terms of order ξ^2 yield the second-order equations.

In order to illustrate the perturbation procedure, consider the strain-rotation equation

$$\epsilon_1 = e_1 + (\chi^2 + \theta^2)/2 \tag{15}$$

Substituting the expansions for each of these variables and dropping terms of order ξ^2 and higher gives

$$\epsilon_1^{(0)} + \xi\epsilon_1^{(1)} + \xi^2\epsilon_1^{(2)} = e_1^{(0)} + \xi e_1^{(1)} + \xi^2 e_1^{(2)} + [\chi^{(0)} + \xi\chi^{(1)} + \xi^2\chi^{(2)}]^2/2 + [\xi\theta^{(1)} + \xi^2\theta^{(2)}]^2/2 \tag{16}$$

In Eq. (16) the prebuckling rotation about the normal direction $\theta^{(0)}$ has been omitted since it is identically zero for an axisymmetric torsionless prebuckling state. The prebuckling rotation $\chi^{(0)}$ is also a function of ξ through its dependence on λ. However, since $a = 0$, it follows that the difference between $\chi^{(0)}(\lambda)$ and $\chi^{(0)}(\lambda_c)$ is $0(\xi^2)$. Consequently, up to the order considered, no error is incurred if $\chi^{(0)}$ is evaluated at $\lambda = \lambda_c$. Subtracting the prebuckling relation $\epsilon_1^{(0)} = e_1^{(0)} + \chi^{(0)2}/2$ from Eq. (16) and equating terms of the same order in ξ gives

$$\epsilon_1^{(1)} - e_1^{(1)} - \chi^{(0)}\chi^{(1)} = 0 \tag{17a}$$

$$\epsilon_1^{(2)} - e_1^{(2)} - \chi^{(0)}\chi^{(2)} = [\chi^{(1)2} + \theta^{(1)2}]/2 \tag{17b}$$

Equation (17a) is one of the field equations for the buckling mode, and (17b) is one of the field equations for the second-order postbuckling state. It should be observed that the homogeneous parts (i.e., the left-hand sides) of these two equations are identical, the only difference being the addition in Eq. (17b) of a nonhomogeneous term quadratically dependent on the buckling mode. This difference is typical of all equations arising from field equations with nonlinear terms. Linear field equations give rise to equations that are identical in form to the original field equation from which they are derived.

Applying this procedure to all of the field equations given in the preceding section yields the following equations for the second-order postbuckling state. The equilibrium equations are identical to the *linearized* form of Eqs. (11) if the load

terms are identified as§

$$X_1 = \lambda_c p\chi - [T_1^{(0)} + T_2^{(0)}]\theta'/r - \{[T_1^{(1)} + T_2^{(1)}]\theta^{(1)}\}'/r \quad (18a)$$

$$X_2 = \lambda_c p\psi - r'[T_1^{(0)} + T_2^{(0)}]\theta/r - r'[T_1^{(1)} + T_2^{(1)}]\theta^{(1)}/r \quad (18b)$$

$$X_3 = \lambda_c[p(e_1 + e_2) + \xi\partial p/\partial x + \eta\partial p/\partial y] \quad (18c)$$

$$L_1 = T_2^{(0)}\psi + T_{12}\chi^{(0)} + T_2^{(1)}\psi^{(1)} + T_{12}^{(1)}\chi^{(1)} \quad (18d)$$

$$L_2 = -T_1^{(0)}\chi - T_1\chi^{(0)} - T_1^{(1)}\chi^{(1)} - T_{12}^{(1)}\psi^{(1)} \quad (18e)$$

The kinematic equations (13), being linear, apply unaltered to the second-order postbuckling state. The strain-rotation equations become

$$\epsilon_1 = e_1 + \chi^{(0)}\chi + [\chi^{(1)2} + \theta^{(1)2}]/2 \quad (19a)$$

$$\epsilon_2 = e_2 + [\psi^{(1)2} + \theta^{(1)2}]/2 \quad (19b)$$

$$\epsilon_{12} = e_{12} + \chi^{(0)}\psi + \chi^{(1)}\psi^{(1)} \quad (19c)$$

The constitutive equations become

$$T_2 = \lambda_{11}\epsilon_2 + \lambda_{12}\kappa_2 + \lambda_{13}T_1 + \lambda_{14}M_1 \quad (20a)$$

$$M_2 = \lambda_{21}\epsilon_2 + \lambda_{22}\kappa_2 + \lambda_{23}T_1 + \lambda_{24}M_1 \quad (20b)$$

$$\epsilon_1 = \lambda_{31}\epsilon_2 + \lambda_{32}\kappa_2 + \lambda_{33}T_1 + \lambda_{34}M_1 \quad (20c)$$

$$\kappa_1 = \lambda_{41}\epsilon_2 + \lambda_{42}\kappa_2 + \lambda_{43}T_1 + \lambda_{44}M_1 \quad (20d)$$

$$2M_{12} = \mu_{11}\kappa_{12}\dagger + \mu_{12}S\dagger \quad (20e)$$

$$\epsilon_{12} = \mu_{21}\kappa_{12}\dagger + \mu_{22}S\dagger \quad (20f)$$

where

$$\kappa_{12}\dagger = \kappa_{12} - \epsilon_{12}/R_2 \quad (21a)$$

$$S\dagger = S - [T_1^{(0)} + T_2^{(0)}]\theta/2 - [T_1^{(1)} + T_2^{(1)}]\theta^{(1)}/2 \quad (21b)$$

Equation (14a) becomes

$$T_{12} = S - 2M_{12}/R_2 - [T_1^{(0)} + T_2^{(0)}]\theta/2 - [T_1^{(1)} + T_2^{(1)}]\theta^{(1)}/2 \quad (22)$$

whereas Eqs. (14b-g), being linear, remain unaltered in form.

A similar analysis can be made on the differential equations for elastic rings. In analogy with Eqs. (18), the resulting equations are identical in form to the linearized ring equations if the applied moments and forces per unit of length are identified as

$$F_x = 0 \quad (23a)$$

$$F_y = -EA[\omega_x^{(1)2} + \omega_y^{(1)2}]/2a \quad (23b)$$

$$F_\phi = EA[\omega_x^{(1)2} + \omega_y^{(1)2}]'/2a \quad (23c)$$

$$N_x = -T_\phi^{(0)}\omega_x - T_\phi^{(1)}\omega_x^{(1)} \quad (23d)$$

$$N_y = -T_\phi^{(0)}\omega_y - T_\phi^{(1)}\omega_y^{(1)} \quad (23e)$$

$$N_\phi = 0 \quad (23f)$$

Method of solution

Examination of the equations of the preceding section shows that all nonhomogeneous terms are quadratic functions of buckling mode variables. Since, in general, these variables are pure harmonic functions of the circumferential coordinate ϕ, the nonhomogeneous terms may be decomposed into an axisymmetric component and a sinusoidal component. This is accomplished by use of the trigonometric identities

$$\cos^2 x = (1 + \cos 2x)/2 \quad (24a)$$

$$\sin^2 x = (1 - \cos 2x)/2 \quad (24b)$$

$$\sin x \cos x = \sin 2x/2 \quad (24c)$$

Denoting the nonhomogeneous parts of the load terms of Eqs. (18) with the superscript (e), and the amplitudes of the buckling mode variables by the same symbols as used previously for total quantities, one obtains

$$X_1^{(e)} = -(n_c/r)[T_1^{(1)} + T_2^{(1)}]\theta^{(1)} \cos 2n_c\phi \quad (25a)$$

$$X_2^{(e)} = -(r'/2r)[T_1^{(1)} + T_2^{(1)}]\theta^{(1)} \sin 2n_c\phi \quad (25b)$$

$$X_3^{(e)} = 0 \quad (25c)$$

$$L_1^{(e)} = (\tfrac{1}{2})[T_2^{(1)}\psi^{(1)} + T_{12}^{(1)}\chi^{(1)}] \sin 2n_c\phi \quad (25d)$$

$$L_2^{(e)} = -(\tfrac{1}{2})[T_1^{(1)}\chi^{(1)} + T_{12}^{(1)}\psi^{(1)}] - (\tfrac{1}{2})[T_1^{(1)}\chi^{(1)} - T_{12}^{(1)}\psi^{(1)}] \cos 2n_c\phi \quad (25e)$$

Similarly, the nonhomogeneous parts of the strain expressions, Eqs. (19), may be decomposed to

$$\epsilon_1^{(e)} = (\tfrac{1}{4})[\chi^{(1)2} + \theta^{(1)2}] + (\tfrac{1}{4})[\chi^{(1)2} - \theta^{(1)2}] \cos 2n_c\phi \quad (26a)$$

$$\epsilon_2^{(e)} = (\tfrac{1}{4})[\psi^{(1)2} + \theta^{(1)2}] - (\tfrac{1}{4})[\psi^{(1)2} + \theta^{(1)2}] \cos 2n_c\phi \quad (26b)$$

$$\epsilon_{12}^{(e)} = (\tfrac{1}{2})\chi^{(1)}\psi^{(1)} \sin 2n_c\phi \quad (26c)$$

The nonhomogeneous term $[T_1^{(1)} + T_2^{(1)}]\theta^{(1)}/2$ in Eqs. (21b) and (22) becomes $(\tfrac{1}{4})[T_1^{(1)} + T_2^{(1)}]\theta^{(1)} \sin 2n_c\phi$, and the nonhomogeneous ring loads become, from Eqs. (23),

$$F_x^{(e)} = 0 \quad (27a)$$

$$F_y^{(e)} = -(EA/4a)[\omega_x^{(1)2} + \omega_y^{(1)2}] + (EA/4a)[\omega_x^{(1)2} + \omega_y^{(1)2}] \cos 2n_c\phi \quad (27b)$$

$$F_\phi^{(e)} = (n_c EA/2a)[\omega_x^{(1)2} + \omega_y^{(1)2}] \sin 2n_c\phi \quad (27c)$$

$$N_x^{(e)} = -(\tfrac{1}{2})T_\phi^{(1)}\omega_x^{(1)} \sin 2n_c\phi \quad (27d)$$

$$N_y^{(e)} = -(\tfrac{1}{2})T_\phi^{(1)}\omega_y^{(1)} \sin 2n_c\phi \quad (27e)$$

$$N_\phi^{(e)} = 0 \quad (27f)$$

It follows, therefore, that the response variables for the second-order post-buckling state are composed of the two harmonics $n = 0$ and $n = 2n_c$, which are uncoupled and may be solved for individually, one after the other. Each of these problems is analogous to a linear shell statics problem with pure sinusoidal loading so that the method of solution presented in Ref. 20 can be used.

For each harmonic, the boundary conditions at meridional stations at which elastic rings are attached may be written in the matrix notation of Ref. 19 as

$$r\Delta\{y\} - [k - \kappa(\lambda_c)]\{z\} = -[e]^T\{L\} \quad (28)$$

where

$$\{L\} = \begin{Bmatrix} aF_x^{(e)} + nN_y^{(e)} \\ aF_y^{(e)} - nN_x^{(e)} \\ aF_\phi^{(e)} - N_x^{(e)} \\ aN_\phi^{(e)} \end{Bmatrix} \quad (29)$$

Here $F^{(e)}$ and $N^{(e)}$ are either the axisymmetric or sinusoidal amplitudes of the corresponding total quantities given by Eqs. (27). Other boundary conditions for the second-order postbuckling state are either homogeneous versions of general linear conditions imposed on the actual shell (e.g., external line loads) or conditions at the initial and/or terminal shell edge representing a spherical dome closure (for details see Appendix A of Ref. 18).

After the solution for the second-order state is obtained, the postbuckling functionals b and K can be computed. The formulas for these quantities, as well as α and β, can be

§ For clarity, the superscript (2) is henceforth omitted from the second-order postbuckling state variables. Terms of Eqs. (18a-c) with the symbol p are associated with a normal pressure field $\lambda p(x,y)$ and are omitted for dead loading.

Table 1 Imperfection sensitivity of 20° clamped spherical shells

Λ	$t/R \times 10^3$	p_c/p_0	b	$K_0R^3/E \times 10^2$	K/K_0	α_{mode}	β/α	$\bar{\delta}/\bar{\xi}t$
6	10.94	0.782(2)	−0.790	5.891	4.195	7.78	0.699	13.45
8	6.16	0.770(4)	−0.963	3.804	5.118	10.18	0.801	16.31
10	3.94	0.778(5)	−1.020	2.496	2.463	14.35	0.482	23.16
12	2.74	0.781(7)	−1.063	1.829	2.347	17.79	0.690	27.73
14	2.01	0.786(9)	−1.071	1.369	2.221	21.21	0.658	32.98
16	1.54	0.790(11)	−1.092	1.067	2.054	25.01	0.646	38.63
18	1.22	0.793(12)	−1.099	0.855	1.765	30.65	0.605	47.56

reduced to integrals over the shell meridian plus algebraic sums over all rings. These formulas are given in Appendix B of Ref. 18 and are not repeated here.

III. Examples

In presenting numerical results for the functionals b, α, β, and K, it should be pointed out that in general their values are not uniquely determined by virtue of the arbitrariness of the manner of normalization of the buckling mode, imperfection shape, and unit load system. In fact, from the general formulas for these quantities,[17] it is easy to see that if the buckling mode, imperfection shape, and unit load system are changed by the multiplicative factors C_1, $\bar{C}$, and C_0, respectively, then b, α, β, and K change by the multiplicative factors C_1^2, $\bar{C}/C_1$, and $1/C_0^2$, respectively. On the other hand, since for a given imperfection, the imperfection amplitude $\bar{\xi} \sim 1/\bar{C}$, it follows, as it should, that the quantities which determine the physical knockdown (Fig. 1), viz., $b\alpha^2\bar{\xi}^2$ and β/α, have unique values, as does also the ratio K/K_0. In order to make the individual quantities have unique values for presentation, in the following examples it will be assumed, except as otherwise explicitly noted, that the buckling mode is normalized to have a normal deflection amplitude equal to the shell thickness; imperfection shapes are normalized to have unit mean square angular amplitudes; and the unit load system corresponds to unit external pressure or unit axial compression, as the case may be.

A. Spherical Caps

Results have been obtained for a 20° (half-angle) clamped spherical cap ($\nu = \frac{1}{3}$) loaded by uniform live pressure for several values of thickness, corresponding to values of the shallow shell rise parameter Λ in the range $6 \leq \Lambda \leq 18$. (For a discussion of the case $\Lambda = 4$, see Ref. 21.) These results are presented in Table 1. Only the harmonic numbers indicated by Huang[22] as being critical for shallow shells have been investigated. These are shown in parenthesis in the critical pressure column. Results are shown only for imperfection shapes proportional to the buckling modes, since in this case there is negligible difference between this shape and the imperfection shape which maximizes α.

The values of b and K/K_0 given are in good agreement with the graphical results presented previously by Fitch and Budiansky.[13] (In Ref. 13 values of α and β were not presented.) From Table 1 and Fig. 1, a plot can be made of the critical load for imperfect shells for various values of $\bar{\xi}$, as shown in Fig. 2. Also shown on this plot are the upper and lower bound experimental values of several investigators.[23] Note that the curves for constant values of $\bar{\xi}$ predict greater imperfection sensitivity for thinner shells, which is in agreement with the trend of the experimental data. On the other hand, the curve shown for $\bar{\delta}/t = 0.1$ goes against this trend. A qualitatively similar result was noted for axisymmetric imperfections of complete spherical shells in Ref. 3, viz., for given values of $\bar{\delta}/t$, thinner shells appear to be less imperfection-sensitive. The fact that the constant $\bar{\xi}$ curves show the same trend as the test data lends support to the hypothesis that $\bar{\xi}$ can be used as a suitable imperfection measure.

The buckling load knockdowns shown in Fig. 2 for $\bar{\xi} = 0.015$ rad range from 0.65 for $\lambda = 6$ to 0.23 for $\lambda = 18$. Since β/α is in the range 0.5–0.8, it is clear from Fig. 1 that consideration of nonzero β has a significant effect on the plot of Fig. 2, at least for the larger values of $\bar{\xi}$. Since the β-terms represent only an incomplete second approximation, one would suspect further significant quantitative changes in the lower part of Fig. 2 if all terms of the order of the β-terms were included in the analysis. It is also interesting to note that the relatively rapid drop in lower bound test data, as λ increases for $\lambda < 10$ as compared with $\lambda > 10$, seems to correlate with the sharp reduction in β/α at $\lambda = 10$ (see Table 1). However, this agreement may well be fortuitous.

B. Stringer-Stiffened Cylindrical Shell

A simply supported cylindrical shell was chosen with $t/r = 0.001343$, $l/r = 0.65$, and $\nu = 0.3$, corresponding to the curvature parameter $Z = 300$. In addition, the following stringer properties were chosen: $EI/Dd = 100$, $A/dt = 1$, and $e/t = 6$ (external stringers). In order to compare with the results of Ref. 15, in which stringer torsional stiffness is neglected, GJ/Dd was set to zero. From Table 2 of Ref. 15, it is seen that the predicted critical harmonic for this shell is exactly $n_c = 10$, so that no error can be attributed to the treatment in that paper of n as a continuous variable. Table 2 compares the present results to those of Ref. 15.

Table 2 Comparison of results for a stringer-stiffened cylinder

	P_c/P_0	b	$\alpha^2 b$	Θ_0	Θ
This paper	8.74	−0.0114	−0.00360	36.4°	−141.1°
Ref. 15	8.79	−0.012	−0.0042	36.	−142.

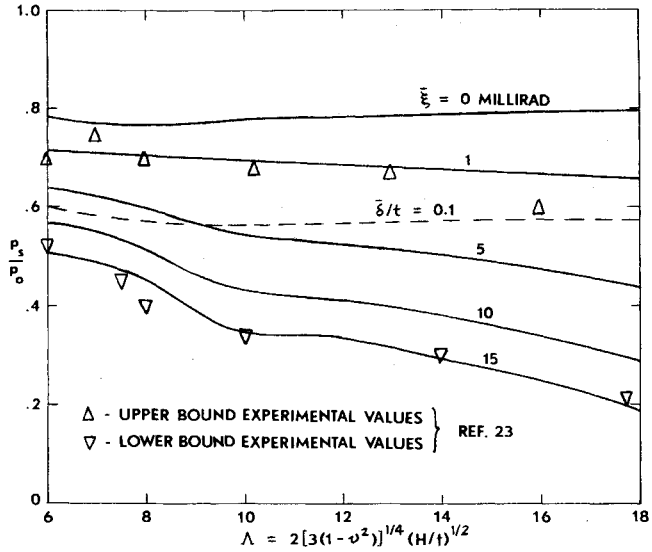

Fig. 2 Critical pressures of imperfect clamped shallow spherical caps.

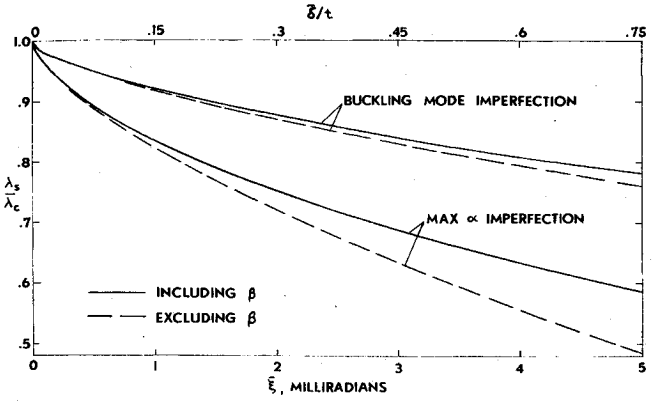

Fig. 3 Stringer-stiffened cylinder (Z = 300, external stringers).

In Table 2, α-values are based on an imperfection shape identical to the normalized buckling mode deflections. As seen, the agreement between the finite-difference results of Ref. 15 and the present results is good except for the imperfection parameter α. In Ref. 24, however, it is noted that this discrepancy is primarily the result of truncation error in the finite-difference solution associated with the use of only 60 finite-difference stations. The convergence of the finite-difference solution for b and $\alpha^2 b$ as the number of stations N increases is shown in Table 3, taken from Ref. 24. These results show that as the number of stations increases, the corresponding finite-difference solution tends to agree better with the present results. Complete numerical agreement, however, can not be expected because of differences between the Donnell shell theory used in Refs. 15 and 24 and the Novozhilov theory used here.

In addition to the results shown in Table 2, the following results were obtained for imperfection shapes normalized to have unit mean square angular amplitudes: for the maximum α imperfection, $\alpha = 267$, $\beta/\alpha = 0.695$; for the buckling mode imperfection, $\alpha = 84.5$, $\beta/\alpha = 0.592$, $\bar{\delta}/\bar{\xi}t = 150$. From these results and Figs. 1, Fig. 3, showing knockdown factors for imperfect shells, was constructed. In contrast to the preceding results for the spherical caps, for given values of $\bar{\xi}$, the buckling mode imperfection is seen to grossly underestimate the full imperfection sensitivity.

C. Prolate Spheroidal Shells

The imperfection sensitivity of unstiffened and ring-stiffened complete prolate spheroidal shells under uniform hydrostatic pressure was evaluated. In Ref. 19 theoretical buckling pressures for each of these shells have been presented and

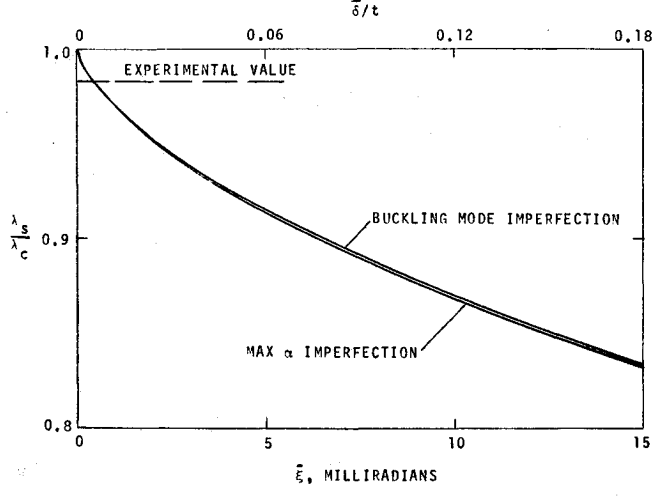

Fig. 4 Unstiffened spheroid (DTMB Model PS-9).

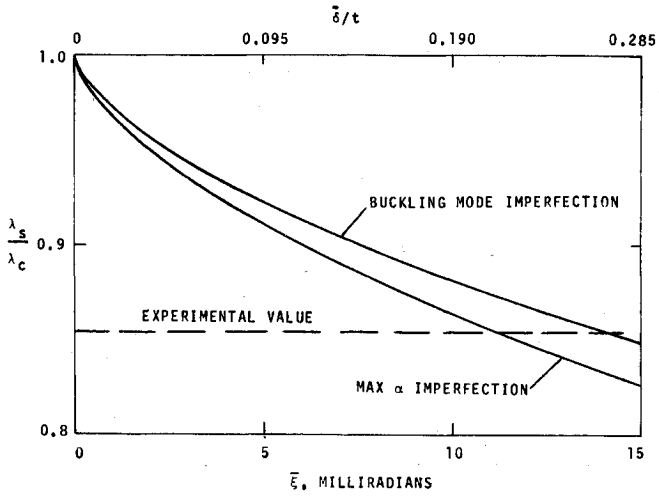

Fig. 5 Ring-stiffened spheroid (DTMB Model SPS-2).

compared to experimental values obtained by Healey.[25] Both shells have a semimajor axis $r_a = 9.0$ in. and a semiminor axis of $r_b = 3.0$ in. and are constructed of epoxy resin with nominal elastic properties of $E = 3.25 \times 10^5$ psi and $\nu = 0.4$.

Unstiffened spheroid

The computed results for this shell with a thickness of 0.189 in. (denoted as model PS-9 in Ref. 25) are $p_c = 139.3$ psi, $b = -0.0300$, $K/K_0 = -0.0338$, $\alpha_{max} = 12.2$, $\alpha_{mode} = 12.0$, and $\bar{\delta}/\bar{\xi}t = 11.9$. In addition, for either type of imperfection, $\beta/\alpha = 1.00$. As in the case of the spherical caps, there is very little effective difference between the "worst" imperfection and the buckling mode imperfection. Furthermore, since $\alpha_{mode}/(\bar{\delta}/\bar{\xi}t) \simeq 1$ (i.e., for an imperfection shape identical to the normalized buckling mode deflections, $\alpha \simeq 1$), and $\beta/\alpha \simeq 1$, it follows that the effects on α and β of nonlinearity in the prebuckling state and prebuckling deformations are negligible. Danielson[14] has studied spheroidal shells parametrically using a membrane prebuckling state. Careful reading of Fig. 5 of Ref. 14 for $r_a/r_b = 3$ and $q = [12(1-\nu^2)]^{1/4}(r_b/t)^{1/2} = 8.13$ gives $b/(1-\nu^2) = -0.0364$. For the shell studied here, $q = 7.10$ and $b/(1-\nu^2) = -0.0357$ Since Danielson's curves indicate that $b/(1-\nu^2)$ increases in absolute value as q decreases, the discrepancy is actually slightly larger than the difference between 0.0364 and 0.0357. Considering that the value of ν used in Ref. 14 is probably different from the value 0.4 used here, this discrepancy is quite acceptable.

From these results and Fig. 1, Fig. 4 was constructed. As seen from this chart, the experimental buckling pressure given in Ref. 25 corresponds to a buckling mode imperfection with a normal amplitude of only 0.005 of the shell thickness or a root mean square amplitude of only 0.5 milliradians.

Ring-stiffened spheroid

The ring-stiffened spheroidal shell (denoted as model SPS-2 in Ref. 25) has 29 equally spaced internal rings, and for this study a shell thickness of 0.087 in. was assumed.¶ The rings

Table 3 Effect of step size on finite-difference solution[24]

N	b	$\alpha^2 b$
30	−0.0130	−0.0052
60	−0.0121	−0.00425
95	−0.0119	−0.00395

¶ In Ref. 19 shell thickness of 0.080 and 0.087 in. were both treated.

have a 0.12-in. square cross section with principal axes parallel to and normal to the axis of revolution, and have a center-to-center spacing of 0.58 in. For both shell and rings, $E = 3.25 \times 10^5$ psi and $\nu = 0.4$. The computed results for this shell are $p_c = 76.15$ psi,** $b = -0.00876$, $K/K_0 = -0.0522$, $\alpha_{\max} = 24.0$, $\alpha_{\text{mode}} = 19.1$, and $\bar{\delta}/\bar{\xi}t = 19.0$. In addition, for either type of imperfection, $\beta/\alpha = 1.00$. As in the case of the unstiffened spheroid, since $\alpha_{\text{mode}} \simeq \bar{\delta}/\bar{\xi}t$ and $\beta/\alpha \simeq 1$, it would appear that linear membrane theory again adequately describes the prebuckling state. This conclusion was also reached in Ref. 19 by direct examination of the prebuckling response. On the other hand, for a given value of the imperfection amplitude $\bar{\xi}$, there is a significant difference between the buckling mode imperfection and the imperfection which maximizes α.

Fig. 5 shows the knockdown factors for this shell based on the preceding results. Comparison of Figs. 4 and 5 shows that, in spite of the greater experimental knockdown for the ring-stiffened model SPS-2, it has roughly the same degree of sensitivity to imperfections as the unstiffened model PS-9. Note that if only buckling mode imperfections are considered and $\bar{\delta}/t$ is used as a measure of imperfections, model SPS-2 appears to be less sensitive than model PS-9. However, as pointed out by Koiter[3] (see also earlier discussion of spherical caps), $\bar{\delta}/t$ is not a suitable imperfection measure since for the thinner shell, SPS-2, the same value of $\bar{\delta}/t$ implies a smaller imperfection. The fact that the experimental knockdown for model SPS-2 was significantly greater than that for PS-9 leads one to believe that this was an isolated result associated with the use of a poorer test specimen for the ring-stiffened shell than for the unstiffened shell.

IV. Concluding Remarks

Based on moderate rotation shell and ring theory, an efficient numerical method for implementing Koiter's unique mode buckling theory for practical shells of revolution has been presented. In addition, in an attempt to enhance the usefulness of the theory, two new quantities have been introduced, viz., the mean square angular imperfection amplitude $\bar{\xi}$ and the second imperfection parameter β. Comparison of theoretical and experimental results for spherical caps tends to support the use of $\bar{\xi}$ as a more appropriate imperfection measure than the usual normal deviation to thickness parameter $\bar{\delta}/t$. In addition, computed values of β for several shells show that, in general, for buckling load knockdowns of roughly 0.6 or less, the effect of β-terms is not negligible. However, the inclusion of β represents only part of an improved approximation to Koiter's general (including nonlinear prebuckling effects) unique mode theory. Therefore, it would be desirable to obtain a complete self-consistent β-approximation. (For further discussion of this question, see Ref. 26.)

It may be noted that the computer program based on the formulation presented is a natural sequel to a buckling program[19] presented previously. Used together, the theoretical buckling modes and their sensitivity to geometric imperfections can be determined for a wide range of practical structures, the analytical evaluation of which, without such programs, would be impossible.

References

[1] Koiter, W. T., "On the Stability of Elastic Equilibrium" (in Dutch), Thesis, 1945, Polytechnic Institute at Delft, H. J. Paris, Amsterdam; English translation, TT F-10,833, 1967, NASA.

[2] Koiter, W. T., "Elastic Stability and Postbuckling Behavior," *Nonlinear Problems*, edited by R. E. Langer, University of Wisconsin Press, Madison, Wis., 1963, pp. 257–275.

[3] Koiter, W. T., "General Equations of Elastic Stability for Thin Shells," *Proceedings, Symposium on the Theory of Shells to Honor Lloyd Hamilton Donnell*, Univ. of Houston, 1967, pp. 187–230.

[4] Budiansky, B. and Hutchinson, J. W., "Dynamic Buckling of Imperfection-Sensitive Structures," *Proceedings of the XI International Congress of Applied Mechanics*, edited by H. Gortler, Springer-Verlag, Berlin, 1964, pp. 636–651.

[5] Budiansky, B., "Dynamic Buckling of Elastic Structures: Criteria and Estimates," *Proceedings, International Conference on Dynamic Stability of Structures*, Pergamon, New York, 1966, pp. 83–106.

[6] Budiansky, B., "Post-Buckling Behavior of Cylinders in Torsion," *2nd I.U.T.A.M. Symposium on the Theory of Thin Shells*, Copenhagen, Denmark, Sept. 5–9, 1967.

[7] Koiter, W. T., "The Nonlinear Buckling Problem of a Complete Spherical Shell Under Uniform External Pressure," Proceedings, Royal Netherlands Academy of Sciences, Amsterdam, Vol. B72, 1969, pp. 40–123.

[8] Hutchinson, J. W., "Imperfection Sensitivity of Externally Pressurized Spherical Shells," *Journal of Applied Mechanics*, Vol. 34, March 1967, pp. 49–55.

[9] Koiter, W. T., "Buckling and Post-Buckling Behavior of a Cylindrical Panel under Axial Compression," Rept. S476, National Aeronautical Research Institute (NLR), Amsterdam, 1956.

[10] Hutchinson, J. W., "Initial Post-Buckling Behavior of Toroidal Shell Segments," *International Journal of Solids Structures*, Vol. 3, 1967, pp. 97–115.

[11] Hutchinson, J. W. and Amazigo, J. C., "Imperfection-Sensitivity of Eccentrically Stiffened Cylindrical Shells," *AIAA Journal*, Vol. 5, No. 3, March 1967, pp. 392–401.

[12] Fitch, J. R., "The Buckling and Post-Buckling Behavior of Spherical Caps under Concentrated Load," *International Journal of Solids Structures*, Vol. 4, 1968, pp. 421–446.

[13] Fitch J. R. and Budiansky, B., "The Buckling and Post-Buckling Behavior of Spherical Caps under Axisymmetric Load," *Proceedings, 10th ASME/AIAA Structures, Structural Dynamics and Materials Conference*, New Orleans, April 1969.

[14] Danielson, D. A., "Buckling and Initial Postbuckling Behavior of Spheroidal Shells under Pressure," *AIAA Journal*, Vol. 7, No. 5, May 1969, pp. 936–944.

[15] Hutchinson, J. W. and Frauenthal, J. C., "Elastic Post-buckling Behavior of Stiffened and Barreled Cylindrical Shells," *Journal of Applied Mechanics*, Vol. 36, 1969, pp. 784–790.

[16] Cohen, G. A., "Imperfection Sensitivity of Optimum Structural Designs for a Mars Entry Capsule," CR (number to be assigned), 1970, NASA.

[17] Cohen, G. A., "Effect of a Nonlinear Prebuckling State on the Postbuckling Behavior and Imperfection Sensitivity of Elastic Structures," *AIAA Journal*, Vol. 6, No. 8, Aug. 1968, pp. 1616–1619; also "Reply by Author to J. R. Fitch and J. W. Hutchinson," *AIAA Journal*, Vol. 7, No. 7, July 1969, pp. 1407–1408.

[18] Cohen, G. A., "Computer Program for Analysis of Imperfection Sensitivity of Ring-Stiffened Shells of Revolution," CR (number to be assigned), 1970, NASA.

[19] Cohen, G. A., "Computer Analysis of Asymmetric Buckling of Ring-Stiffened Orthotropic Shells of Revolution," *AIAA Journal*, Vol. 6, No. 1, Jan. 1968, pp. 141–149.

[20] Cohen, G. A., "Computer Analysis of Asymmetrical Deformation of Orthotropic Shells of Revolution," *AIAA Journal*, Vol. 2, No. 5, May 1964, pp. 932–934.

[21] Cohen, G. A., "Buckling of Clamped and Simply Supported Shallow Spherical Shells," *AIAA Journal*, Vol. 7, No. 12, Dec. 1969, pp. 2346–2347.

[22] Huang, N. C., "Unsymmetrical Buckling of Thin Shallow Spherical Shells," *Journal of Applied Mechanics*, Vol. 31, Sept. 1964, pp. 447–457.

[23] Krenzke, M. A. and Kiernan, T. J., "Elastic Stability of Near-Perfect Shallow Spherical Shells," *AIAA Journal*, Vol. 1, No. 12, Dec. 1963, pp. 2855–2857.

[24] Hutchinson, J. W., private Communication, Oct. 1969, Harvard Univ., Cambridge, Mass.

[25] Healey, J. J., "Parametric Study of Unstiffened and Stiffened Prolate Spheroidal Shells under External Hydrostatic Pressure," Rept. 2018, Aug. 1965, David Taylor Model Basin.

[26] Cohen, G. A., "Imperfection Sensitivity of Elastic Structures: The Second Approximation for Unique Mode Buckling," presented at the Lockheed Conference on Computer-Oriented Analysis of Shell Structures, Palo Alto, Aug. 1970.

** This value of critical pressure differs slightly from the corresponding value (75.9 psi) reported in Ref. 19 because in this study the ring centroidal eccentricities relative to their point of attachment on the shell reference surface were taken to be radial, whereas in Ref. 19 they were assumed to be normal.